Journal of Innovative Optical Health Sciences
Vol. 8, No. 3 (2015) 1541001 (6 pages)

DOI: 10.1142/S1793545815410011

World Scientific
www.worldscientific.com

Features of structure of external layer of murine hair at different stages of malignant tumor development

Valeriya S. Maryakhina*,‡, Larisa S. Scheglova*
and Ksenia A. Anenkova†
*Institute of Micro- and Nanotechnologies
Orenburg State University
13 Pobedy st., Orenburg 460018, Russia
†Molecular Physics Department
M. V. Lomonosov Moscow State University
1 Leninskiye Gory, Moscow 119991, Russia
‡v.s.maryakhina@gmail.com

Received 26 February 2014
Accepted 24 March 2014
Published 29 April 2014

In the paper, the results of experimental investigations on the differences of wool structure of healthy mice and mice with malignant tumor(s) are represented. It is shown that destruction of wool structure happens during pathology development. Quantity of cells of external wool layer and their thickness decrease when the tumor capsule enlarges. Difference is seen even when the tumor is small. The obtained results can be used to improve optical techniques of biomedical diagnostics of cancer diseases.

Keywords: Breast cancer; hair; optical biomedical diagnostics; atomic force microscopy; dynamic light scattering.

1. Introduction

The optical techniques of biomedical diagnostics are used for detection of biotissue pathological states due to their noninvasiveness and high sensitivity to pathology. However, all these techniques allow to detect tumor when metastases have appeared. According to that, it is essential to raise the accuracy of the optical methods. Parameters, which are significantly different for health and tumor cells, should be found. It can be carried out by either device improving or research object change.

Biotissues and somatic cells are widespread objects for the optical biomedical diagnostics but their significant heterogeneity together with high scattering light[1] significantly complicate obtaining statistically reliable data. That is why new research objects are needed.

In this work, we show the possibility of using hair for optical biomedical diagnostics because of

difference in their structure in normal and pathological states.

2. Objects and Methods of Research

2.1. *Objects of research*

The object of the research was wool of mice (line BYRB) with spontaneous cancer tumors of mammary gland. The wool had been cut from the entire skin surface of healthy mice and mice with malignant tumor(s) of same line. Additionally, we had also carried out experiments with wool from skin located above cancer tumor only. Diameter of tumor capsule was from 1 cm to 3 cm. The wool aliquot was previously cleared twice in medical alcohol. To obtain reliable results, not less than 15 female mice were used for each type of samples.

2.2. *Optical microscopy*

The cleared wool was placed on the slide. Wool structure was investigated by optical inverted microscope Altami invert 3 with video camera working in phase contrast mode (magnification x400).

2.3. *Spectrophotometry*

The cleared wool aliquots were placed into collagenase solution (0.5 mg/mL) in phosphate buffer (pH = 7.4) and were incubated at 37°C for 40 min. The obtained suspension (collagenase with dissolved cells and peptides) was investigated by spectrophotometry. Absorption spectra were measured by spectrofluorimeter SOLAR CM-2203 working in photometric mode. Registration of spectra was carried out respectively of collagenase solution in UV region.

2.4. *Atomic force microscopy*

The cells' structure was investigated by scanning in the atomic-force microscope (AFM) CMM-2000. For that, the obtained cell suspension was cleared twice from collagenase molecules by centrifuging at 6000 rpm for 5 min. The separated cells were placed on mica for measuring. The AFM images in air were obtained using triangular cantilevers (rigidity 0.01 N m^{-1}) with a pyramidal tip having a radius of curvature $r \sim 15$–25 nm.

2.5. *Dynamic light scattering*

Samples were prepared as well as for spectrophotometry. The obtained cell suspension was placed in "Photocor complex" for measuring cells' size. Laser wavelength was 647 nm, the power was 25 mW. Each measurement was during 10 min. For statistical adequacy, the represented results are average of ten or more measurements.

3. The Results and Discussion

It is known[2] that hair of both animals and people has a layered structure. The external layer has connective tissue cells. Next, two internal Henley and Huxley layers consist of keratinized cells with irregular shape. The internal layer is the hair shaft. In spite of the complex multilayer structure, hair can be a health indicator sometimes.[3] Any changes in metabolic processes lead to change in wool's biochemical composition. As a rule, its destruction starts from the external layer. Photo samples of the wool of healthy female mice and females with spontaneous cancer tumor of mammary gland are presented in Fig. 1. As you can see, disturbance of

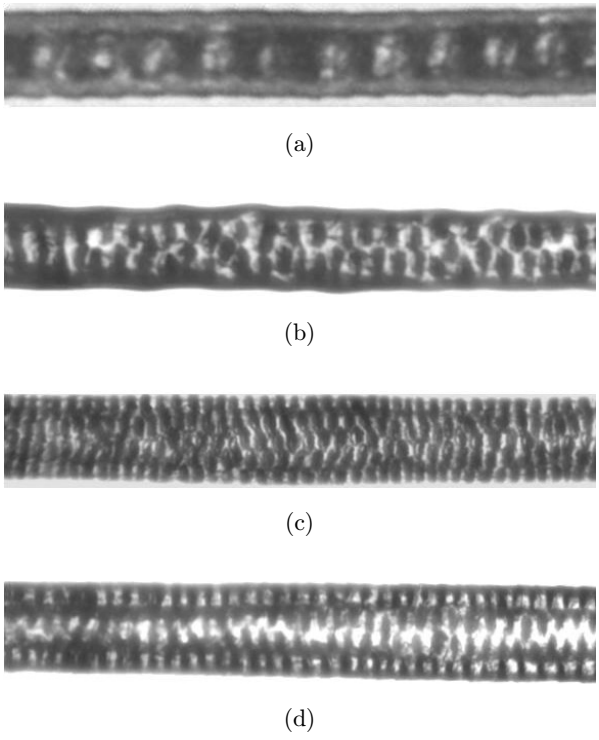

Fig. 1. Wool structure of healthy mouse (a) and mice with cancer tumor 1 cm (b), 2 cm (c) and 3 cm (d). Magnification x400.

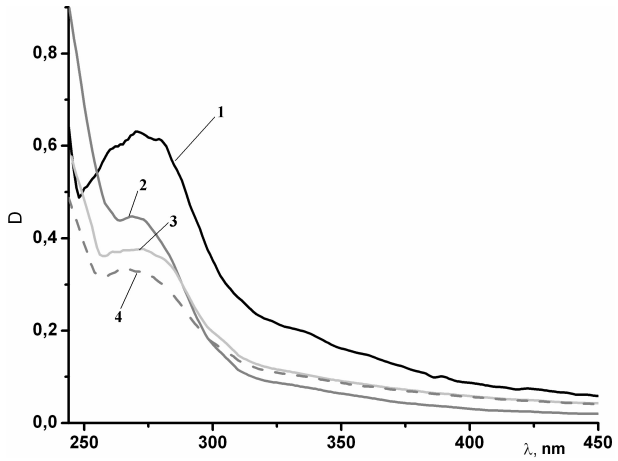

Fig. 2. Absorption spectra of supernatant of wool samples obtained from healthy mouse (1) and from mice with cancer tumor 1 cm (2), 2 cm (3) and 3 cm (4).

hair structure is traceable in sequential stages. Wool of healthy mouse has dense structure, external layer is pronounced. At the same time, wool of mice with cancer tumor is thinner, external and internal layers are destroyed. Difference is even when tumor diameter is small.

The described changes lead to absorption spectra changes (Fig. 2). Treatment with collagenase is used for extracellular matrix degradation and cell separation. Finally, supernatant contains collagenase and dissolved cells after treatment by the enzyme. As you can see from Fig. 2, a serial decrease in optical density of supernatant is and their maxima spectra shift to short-wave region. It is a result of hair structure destruction with pathology development, where cells' number decrease. We can also assume that the internal layer of wool from mice with cancer tumor is destructed too during collagenase treatment. In this case, the absorption spectrum is the result of absorption of two cell layers with different extinction coefficients. We note that no maximum characterizing porphyrins at 420–450 nm is in the absorption spectra. The maximum, however, was observed during *in vitro* experiments with the mice line.[4] It can be connected with no accumulation of porphyrins in their hair structure.

In addition to the decrease of cell quantity in the external layer, its thinning was observed. These data can be presented by scans of external layer wool cells carried out by AFM. Their thickness decrease from 180 nm for healthy mice to 132 nm for mice with large tumor. Cell size is nearly 560 nm for healthy mice and 430/360 nm for mice with tumor 1 and 3 cm, respectively.

These data were confirmed by dynamic light scattering (DLS) method. The DLS method allows to determine the translation diffusion coefficient of disperse particles in a fluid through the analysis of the characteristic time of fluctuations of the scattered light intensity.[5,6] The chaotic Brownian motion of dispersed particles causes microscopic fluctuations in their local concentration. These fluctuations, in turn, lead to local inhomogeneities of the refractive index. The passage of a laser beam through the medium means that part of the light is scattered on these inhomogeneities; the fluctuations of the intensity of the scattered light correspond to fluctuations of the dispersed particles' local concentration.

The dynamic information in the particles is derived from autocorrelation of the intensity trace recorded during the experiment. The autocorrelation function describes the relationship between the signal at the delay time τ and $\tau + d\tau$ as follows:

$$G(t) = \langle I(t) \cdot I(t+\tau) \rangle, \tag{1}$$

where τ is the delay time and I is the density.

This technique is named photon correlation spectroscopy and it is also known as quasielastic light scattering.[5,6]

In the case of a mono-dispersed solution, that contains spherical noninteracting particles of the same size, it is possible to show that the photocurrent power spectrum has the form of a Lorentzian curve[5] with half width Γ. The normalized intensity correlation function is described by an exponential with relaxation time $\tau_{\text{rel}} = 1/\Gamma$ as

$$g_1(\tau) = \exp(-\Gamma t). \tag{2}$$

The decay rate Γ is related to the physical properties of the particles and the experimental conditions by the following expressions:

$$\Gamma = D_t q^2, \tag{3}$$

$$D_t = \frac{kT}{6\pi\eta R}, \tag{4}$$

$$q = k_i - k_s = \left(\frac{4\pi n}{\lambda}\right) \sin\frac{\theta}{2}, \tag{5}$$

where k_i is the wave vector of incident radiation, k_s is the wave vector of scattered radiation, D_t is the translational diffusion coefficient of particles, n is the refractive index of a medium, λ is the scattered

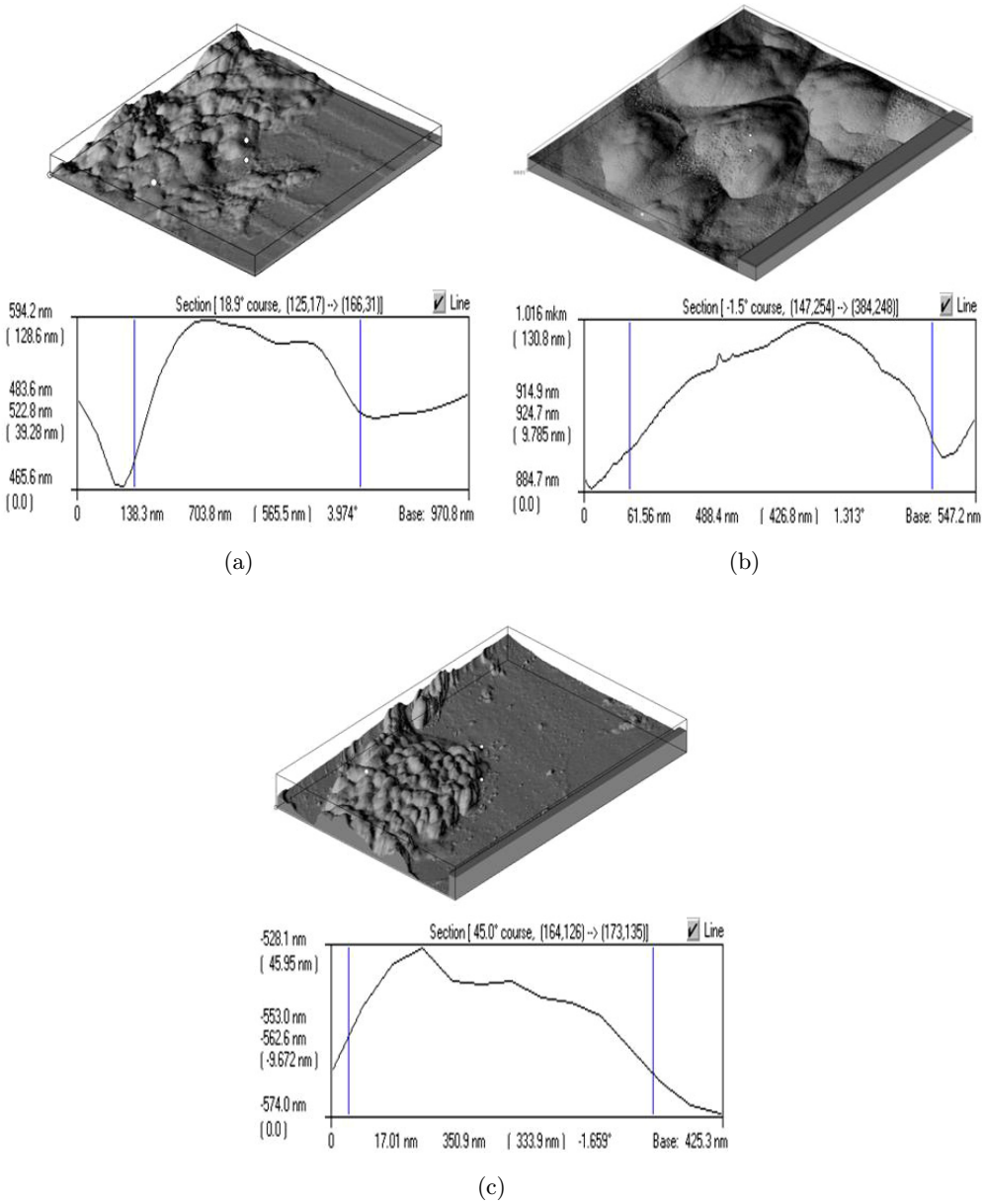

Fig. 3. AFM pictures of external wool layer of healthy mice (a) and mice with small (b) and large (c) tumor.

light wave length, θ is the scattering angle, T is the absolute temperature of the scattering solution, K is the Boltzmann's constant, η is the solvent viscosity and R is the hydrodynamic radius of a particle.

In the case of polydisperse solutions with different sizes of particles, the photocurrent spectrum is a continuous set (integral) of Lorentzian curves with different half widths. Therefore, to find the size distribution of particles (diffusion coefficients); it is necessary to solve the inverse spectral problem in the form of an integral equation with the Lorentzian kernel:

$$g^{(2)}(t) = (g^{(1)}(t))^2 + 1 + \zeta(t); \tag{6}$$

$$g^{(1)}(t) = \int_0^\infty P(\Gamma)\ \exp(-\Gamma t)\ d\Gamma, \tag{7}$$

where $g^{(1)}(t)$ is the normalized autocorrelation function of a signal, $g^{(2)}(t)$ is the normalized autocorrelation function of intensity and $\zeta(t)$ is an error associated with the stochastic nature of the signal itself rather than with the inaccuracy of photocurrent measurement or the noises of a recording channel.[5,7]

Table 1. Cells radius of external wool layer and their diffusion coefficients.

Normal wool		$d_{\text{tumor}} = 1\,\text{cm}$		$d_{\text{tumor}} = 3\,\text{cm}$	
R, nm	$D_t \cdot 10^{-8}$, cm^2/s	R, nm	$D_t \cdot 10^{-8}$, cm^2/s	R, nm	$D_t \cdot 10^{-8}$, cm^2/s
776 ± 146	$0{,}28 \pm 0{,}06$	495 ± 83	$0{,}44 \pm 0{,}07$	368 ± 74	$0{,}59 \pm 0{,}13$
199 ± 36	$1{,}1 \pm 0{,}2$	126 ± 13	$1{,}7 \pm 0{,}2$	99.4 ± 13	$2{,}7 \pm 0{,}4$

Equation (7) is known as the Siegert relation, and will allow one to calculate $g^{(1)}(t)$ in terms of $g^{(2)}(t)$ accumulated by a correlator in the course of an experiment. Integral Eq. (3) forms the main principle of data processing in the method of photon correlation spectroscopy.

The results of our experiments were processed using the DYNALS package of programs, in which the approximate solution (3) was sought by the Tikhonov regularization method for integral equations.[8]

The results of calculations are presented in Table 1. As you can see, each sample contains two cell types. These cell types have different sizes. We assume that it connects on partial separation of Henley layer during collagenase treatment. With pathology process development, cells size decrease for both cell types. We note that the difference between wool cell size of normal and with small tumor mice are nearly 36% for two cell types. Consequently, these distinctions are statistically significant. We do not observe difference in the results after investigation of wool cut from all skin surface and from cancer tumor only for all mice types.

4. Conclusion

Although biomedical diagnostics methods are present, a search for methods of the earlier diagnostics of cancer diseases took us to, for example, Ref. 9 where a method of breast cancer diagnostics based on wool structure investigation by X-rays was proposed. Later investigations[10,11] had not confirmed these data. Nonetheless, research on the wool structure for diagnostics applications are carrying on [see, for instance, 12].

The biological tissue cells are objects with very specific inhomogeneous structure. Effectivity of photoprocesses happening inside the cells depends on the composition of intracellular structures, composition of cell membrane, etc. In turn, the physical-chemical composition of the cells received from pathogenic tissues depends on the stage of pathological process development.[4] It leads to change in the spectral- luminescent properties of cells obtained from tumor at different stages of pathology as well as photosensitizers located within it.[13,14] Taking into account this, the represented data about wool structure can be used to improve the optical techniques for noninvasive diagnostics of cancer diseases at different stages of pathology.

Acknowledgment

The work was partially supported by grant of Ministry of science and education of RF No. 2.338.2011.

References

1. V. V. Tuchin, "Light scattering study of tissues," *Phys. Usp.* **40**, 495–515 (1997).
2. Th. Schlake, "Determination of wool structure and shape," *Seminars in Cell & Dev. Biol.* **18**, 267–273 (2007).
3. S. B. Park, S. W. Choi, A. Y. Nam, "Wool tissue mineral analysis and metabolic syndrome," *Biol. Trace Elem. Res.* **130**, 218–228 (2009).
4. L. S. Scheglova, L. L. Abramova, V. S. Maryakhina, "Optical diagnostics of tumor cells at different stages of pathology development," *Quantum Electron.* **43**, 1088–1090 (2013).
5. G. Z. Kammins, E. R. Paik, *Photon Correlation and Light Beating Spectroscopy*, Plenum, New York (1974).
6. R. Pecora, *Dynamic Light Scattering from Macromolecules*, Stanford Univ., Stanford (1984).
7. K. A. Anenkova, G. P. Petrova, V. V. Gibizova, L. A. Osminkina, K. P. Tamarov, "Optical properties of serum albumin water solutions, containing mesoporous silicon particles," *Optics Spectrosc.* **115** 166–170 (2013).
8. A. V. Ershov, A. I. Mashin, I. A. Karabanova, *Investigation of Vibrational Properties of Amorphous Silicon by the IR Spectroscopy Method: Laboratory Work on the Course Physics of Amorphous and*

Nanocrystalline Semiconductors, NNGU, Novgorod (2007) [in Russian].
9. V. James, J. Kearsley, T. Irving, Y. Amemiya, D. Cookson, "Using wool to screen for breast cancer," *Nature* **398**, 33–34 (1999).
10. F. Briki, B. Busson, B. Salicru, F. Estève, J. Doucet, "Breast-cancer diagnosis using wool," *Nature* **400**, 226 (1999).
11. M. Hart, "Using wool to screen for breast cancer," *Synchrotron Rad. News* **12**, 31–37 (1999).
12. Q. Pasha, S. A. Malik, N. Shaheen, M. H. Shah, "Investigation of trace metals in the blood plasma and scalp wool of gastrointestinal cancer patients in comparison with controls," *Clini. Chim. Acta* **411**, 531–539 (2010).
13. E. L. Abel, J. M. Angel, K. Kiguchi, J. DiGiovanni, "Multi-stage chemical carcinogenesis in mouse skin: Fundamentals and applications," *Nat. Protocols* **4**, 1350–1362 (2009).
14. V. S. Maryakhina, S. N. Letuta, "Pathology development stage and its influence to the delayed fluorescence kinetics of molecular probes," *Laser Phys.* **23**, 025604 (2013).